ARTICLE OPEN

Check for updates

Extracellular vesicle profiling reveals novel autism signatures in patient-derived forebrain organoids

Isidora Stankovic[1], Phillip Smit[2], Jonathan Cross[3], Alin Rai[3], Paul Wolujewicz[1,2,4], David Greening[3,5,6] and Dilek Colak[1,7]✉

Autism Spectrum Disorder (ASD) affects 1 percent of the world's population with an increased prevalence of 178 percent since 2000. Although altered synaptic function putatively accounts for many of the abnormalities seen in ASD, the specific molecular mechanisms underlying this disorder remain poorly defined. A growing body of evidence suggests that extracellular vesicles (EVs), specifically exosomes, play a critical role in cellular communication within the brain. While they have been implicated in various types of diseases from cancer to neurodegeneration, their involvement in ASD remains largely unexplored. In this study, we utilized patient-derived cortical organoid models to characterize EVs secreted by human three-dimensional (3D) tissue and defined their cargo. Our study reports, for the first time, alterations in ASD organoid-derived EVs in comparison to healthy control cortical EVs. By utilizing small RNA sequencing, proteomics, nanoparticle tracking and microscopy, we provide a comprehensive characterization of the cargo carried by EVs secreted from human 3D forebrain models. Our findings reveal substantial differences both in the RNA and protein content of ASD-derived EVs, providing insight into disease mechanisms as well as highlighting the potential of exosome-based diagnostics and therapies for ASD.

Translational Psychiatry (2025)15:393 ; https://doi.org/10.1038/s41398-025-03607-w

INTRODUCTION

Autism Spectrum Disorder (ASD) is a developmental disability characterized by impaired social communication, restrictive repetitive behaviors, and quite often, cognitive deficits [1]. ASD affects 1 in 36 children alone in the US, with a gender ratio of 4:1 affecting boys- a more than fourfold increase since 2000 [2]. ASD is diagnosed using standardized assessment tools such as the Autism Diagnostic Observation Schedule (ADOS) in accordance with the criteria outlined in the Diagnostic and Statistical Manual of Mental Disorders (DSM-5) [1, 2]. After half a century of studying ASD, we have yet to fully understand the initial insults, progression and pathophysiology of this disease, and therefore lack an effective treatment. Approximately 95% of these diagnoses are idiopathic, indicating the absence of a known genetic anomaly [3, 4]. Genome-wide association and animal-model studies from syndromic ASDs suggest that dysregulated synaptic function accounts for most of the abnormalities found in ASD. A combination of factors - genetic abnormalities [2, 3], epigenetics [4, 5], immune system dysfunction [6, 7], maternal immune activation [8–10], and electrophysiological changes [11, 12] have been implicated in the etiology of ASD [13–15]. Current treatments ranging from stem cell therapies to behavioral interventions, are only helpful in a portion of patients [2], and typically consist of a combination of behavioral therapies and interventions aimed to reduce symptoms that interfere with the quality of life [16]. Given the brain's cellular diversity and complexity, manipulating a single cell type is unlikely to yield effective therapeutic outcomes.

The majority of ASD cases exhibit polygenic susceptibility and involve coordinated cell communication amongst multiple cell types [17–20]. Over the last decade, extracellular vesicles (EVs) have been identified as critical players in cell-to-cell communication [21] where they are produced by virtually all cell types and are released into the extracellular environment [21–23]. To date, three main types of vesicles have been characterized: apoptotic bodies (500–2000 nm), microvesicles (50–1000 nm), and exosomes (40–200 nm). Although EVs differ in size, function, and biogenesis [21–23], all are secreted, carry molecules, and are involved in both short and long-distance cellular communication [24, 25]. Additionally, EVs can cross the blood–brain barrier (BBB), and be detected peripherally, making them intriguing candidates in neurodevelopmental biomarker discovery [25], with recent evidence implicating a role for EVs during critical periods of brain development [20–25].

The smallest class of EVs are exosomes ranging from 40–200 nm in size and carry cargo composed of mainly proteins and microRNAs [21]. Exosomes stimulate recipient cells through endocytosis and endosome fusion, direct release of cargo content, and signaling through cell surface receptors [23]. Virtually all cell types in the brain release exosomes, including neurons, astrocytes, microglia, oligodendrocytes, and endothelial cells [25–32]. Neurons and glia have been reported to release exosomes in vitro and

[1]Center for Neurogenetics, Feil Family Brain and Mind Research Institute, Weill Cornell Medicine, Cornell University, New York, NY, USA. [2]Department of Medical Sciences, Frank H. Netter School of Medicine, Quinnipiac University, North Haven, CT, USA. [3]Baker Heart and Diabetes Institute, Melbourne, VIC, Australia. [4]Department of Biomedical Sciences, School of Health Sciences, Quinnipiac University, Hamden, CT, USA. [5]Baker Department of Cardiovascular Research, Translation and Implementation, La Trobe University, Bundoora, VIC, Australia. [6]Baker Department of Cardiometabolic Health, University of Melbourne, Melbourne, VIC, Australia. [7]Gale and Ira Drukier Institute for Children's Health, Weill Cornell Medicine, Cornell University, New York, NY, USA. ✉email: dic2009@med.cornell.edu

Received: 1 May 2025 Revised: 23 July 2025 Accepted: 1 September 2025
Published online: 10 October 2025

in vivo [33–37]. Trophic support of neurons from oligodendrocytes and astrocytes is thought to be conveyed by exosomes [35]. Current evidence for exosome signaling in the brain points toward their role in transcriptional regulation [38], neurogenesis [39, 40], synaptic plasticity [41, 42], and neuroinflammation [43, 44].

While studies found that cargo composition of exosomes is altered in diseases such as cancer and neurodegenerative disorders [22, 45, 46] exosome pathology in neurodevelopmental disorders is yet to be defined. A recent study examined exosomes from frozen *postmortem* prefrontal cortex and detected miRNA alterations in Schizophrenia and bipolar disorder [46]. Exosomes have been shown to both carry hyperphosphorylated Tau between neurons and could seed amyloid-β aggregation in Alzheimer's Disease [47, 48]. In vivo studies demonstrated that the transmission of Tau via microglia-derived exosomes was more efficient than the transmission of the naked form of Tau [49]. Recent studies have also used exosomal alpha-synuclein as a novel biomarker of early-onset Parkinson's disease [50].

Although exosome research in neurodevelopmental disorders is still in its early stages, studies have implicated exosome dysfunction in ASD. In a 2D human cell culture model of Rett syndrome generated by MECP2-knockdown, it was shown that exosomes of MECP2-deficient cells lack proteins crucial for neuronal circuit development, while control exosomes were significantly enriched in proteins important for proliferation, neuronal development, and synaptic maturation [51]. Treatment of MECP2-knockdown cultures with control exosomes rescued the defects in neuronal growth and differentiation [51]. A similar study evaluated the efficacy of stem cell-derived exosomes on ameliorating autism-related behaviors in a BTB3 mouse model of idiopathic autism [52]. Mice treated with exosomes either intranasally or intravenously showed increased social interactions and decreased repetitive behaviors 3 weeks after treatment. A later study administered stem cell-derived exosomes intranasally to a ShankB3 mouse model of autism and observed improvements in vocalization and repetitive behavior phenotypes, as well as increases in GABA receptor GABARB1 expression [53]. While different studies highlight the ability of exosomes to improve autism-related behavioral phenotypes both in idiopathic and syndromic mouse models of ASD, the exact EV pathology and how it may contribute to disease initiation or progression are ill defined.

The emergence of induced pluripotent stem cell (iPSC) technology to derive monolayer brain cell types and 3D brain organoids from human donors offers a unique opportunity to study exosome pathology in ASD [54]. Previously, iPSCs-derived cerebral organoids were used to study the neuropathologies of ASD and schizophrenia during early brain development [55–58]. In the present study, we demonstrate successful isolation and characterization of EVs from ASD patient-derived forebrain organoids. We have identified significant alterations in the RNA and protein cargo of ASD EVs in comparison to healthy control EVs. Altered gene expression in EVs pointed towards disruptions in polyol pathways, protein synthesis, ubiquitination, and chromatin remodeling, all of which are linked to synaptic plasticity, cellular signaling, and protein homeostasis. Intriguingly, we identified several known ASD risk genes among the differentially regulated RNAs and proteins in EVs derived from ASD forebrain organoids. Our findings provide novel insights into the molecular mechanisms of ASD and supports the potential of EVs as therapeutic targets for the disorder.

RESULTS

EVs secreted from CTRL and ASD organoids display similar density and morphology

To characterize EVs in early ASD brain development, we generated 3D dorsal forebrain organoids from human iPSCs. We sampled organoids from 16 unique human donors, comprising $n = 8$ healthy controls (CTRL) and $n = 8$ individuals with ASD (Fig. 1a). Briefly, iPSCs from human donors were grown as monolayer cultures atop vitronectin-coated plates before being dissociated with Accutase to yield single-cell iPSC suspensions. Stem cell suspensions were correspondingly cultured into 3D embryoid bodies before being subjected to Cortical Differentiation Medium (CDM) and maintained as previously described [59]. All 16 lines employed in the study formed organoids of similar morphologies (Fig. 1b), but ASD-derived organoids were significantly larger in diameter than CTRLs (Fig. 1b, c, Fig. S1a). The ASD forebrain organoids exhibited similar phenotypes of increased progenitor pool and reduced neurogenesis as previously reported in this model system as well as in patients (Fig. 1d, e, Fig. S1b-c) (see Discussion).

We next sought to determine whether EVs in ASD organoids are altered compared to EVs secreted by CTRL organoids. The schematic of experimental design and timeline is depicted in Fig. 1a. To study ASD organoid-derived EVs, we generated CTRL and ASD organoids and collected the supernatant at day 60 of in vitro differentiation (60 DIV). Ten days prior to supernatant collection, FBS was removed from media to prevent contamination with FBS-derived vesicles (Fig. 1a). EVs were isolated from culture media using a combination of commercially available kits (ThermoFisher) and ultracentrifugation. To validate EV purification, we followed the guidelines of the International Society for Extracellular Vesicles that recommends nanoparticle tracking analysis (NTA) for biophysical features, transmission electron microscopy (TEM) for high resolution imaging, and Western blot for validation of EV-specific proteins [60, 61] (Fig. 2a). Western blot analysis verified the presence of exosomal markers CD9 and CD63 in the EV pellet post kit precipitation, but not in the processed supernatant sample, pointing to efficient EV isolation (Fig. 2b). NTA revealed that across 16 lines, the majority of particles were < 400 nm (Fig. 2c), with average particle sizes in the 90–250 nm range, representative of exosome size. NTA also allowed us to measure EV concentrations across samples. Intriguingly, ASD EVs and CTRL EVs did not differ in either size or density (Fig. 2d). To visualize organoid-derived EVs, we employed TEM as previously described [61, 62]. TEM images revealed vesicles exhibiting cup/rose-like morphologies, commonly associated with exosomes (Fig. 2e). Taken together, we have used three techniques that independently assessed the size, morphology, or biochemistry of vesicles isolated from ASD and CTRL forebrain organoids. Although these analyses collectively suggest that the isolated EVs are mainly composed of exosomes, we cannot exclude the possibility that we have also isolated other types of EVs along with exosomes. Therefore, we simply refer to the purified vesicles as EVs.

RNA and protein profiles are significantly different between ASD and CTRL EVs

To compare the small RNA profiles of EVs derived from CTRL organoids and ASD organoids, we employed small RNA sequencing using the NEXTFLEX Small RNA Sequencing kit v4 which is designed to capture short RNAs (17–65 nucleotides) with 5′ monophosphorylated and 3′ hydroxylated ends. However, the kit also allows for the capture of larger molecules (< 200 bp) by using the no-size selection protocol. We were able to detect RNAs from all 16 lines used in the study with dispersion estimate signifying low read count bias (Fig. S2a). Of note, one line (CTRL line 3) showed low levels of RNA abundance (Fig. S2b) and thus was excluded from downstream analysis. We first assessed RNA types present in the purified EVs and determined that organoid-derived EVs carry a large RNA heterogeneity. We incorporated the cut-off of 50 base pairs early in our pipeline and into the alignment steps. Intriguingly, in addition to non-coding RNAs, the analysis revealed that many of the fragments consistently aligned to protein coding

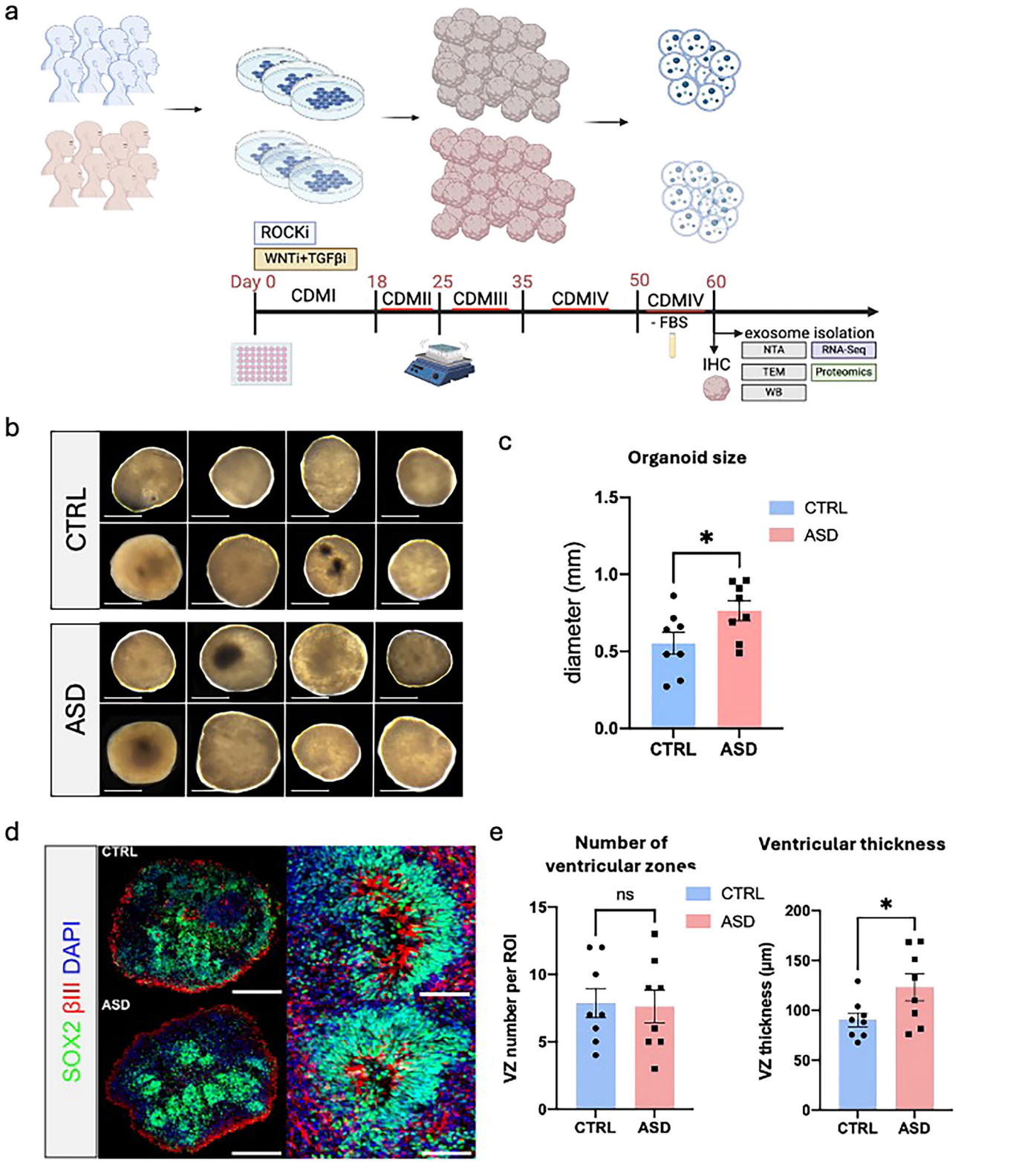

Fig. 1 Forebrain organoids generated from iPSC lines derived from healthy controls and individuals with ASD. a Schematic depicting experimental design and timeline. Briefly, forebrain organoids were generated using a previously described protocol [59]. At 60 DIV, media was collected, and EVs were isolated, followed by subsequent analysis. **b** Light microscopy images of representative brain organoids at 60 DIV from all 16 lines used in the study. **c** Bar graph depicts average size of organoids derived from CTRL and ASD lines ($n = 8$ lines per group; $n = 3$ organoids per line; Student's t-test). **d** Representative images of SOX2 (green), β-III-tubulin (red) and DAPI (blue) immunostaining in CTRL and ASD organoids to assess proliferative and neurogenic zones. **e** Quantifications of ventricular-like zone density and thickness across 16 organoid lines used in the study ($n = 8$ lines per group; $n = 3$–10 organoids per line). Scale bar = 0.25 mm in b; 500 µm in d. Data is represented as mean ± SEM, $p < 0.05$, Student's t-test.

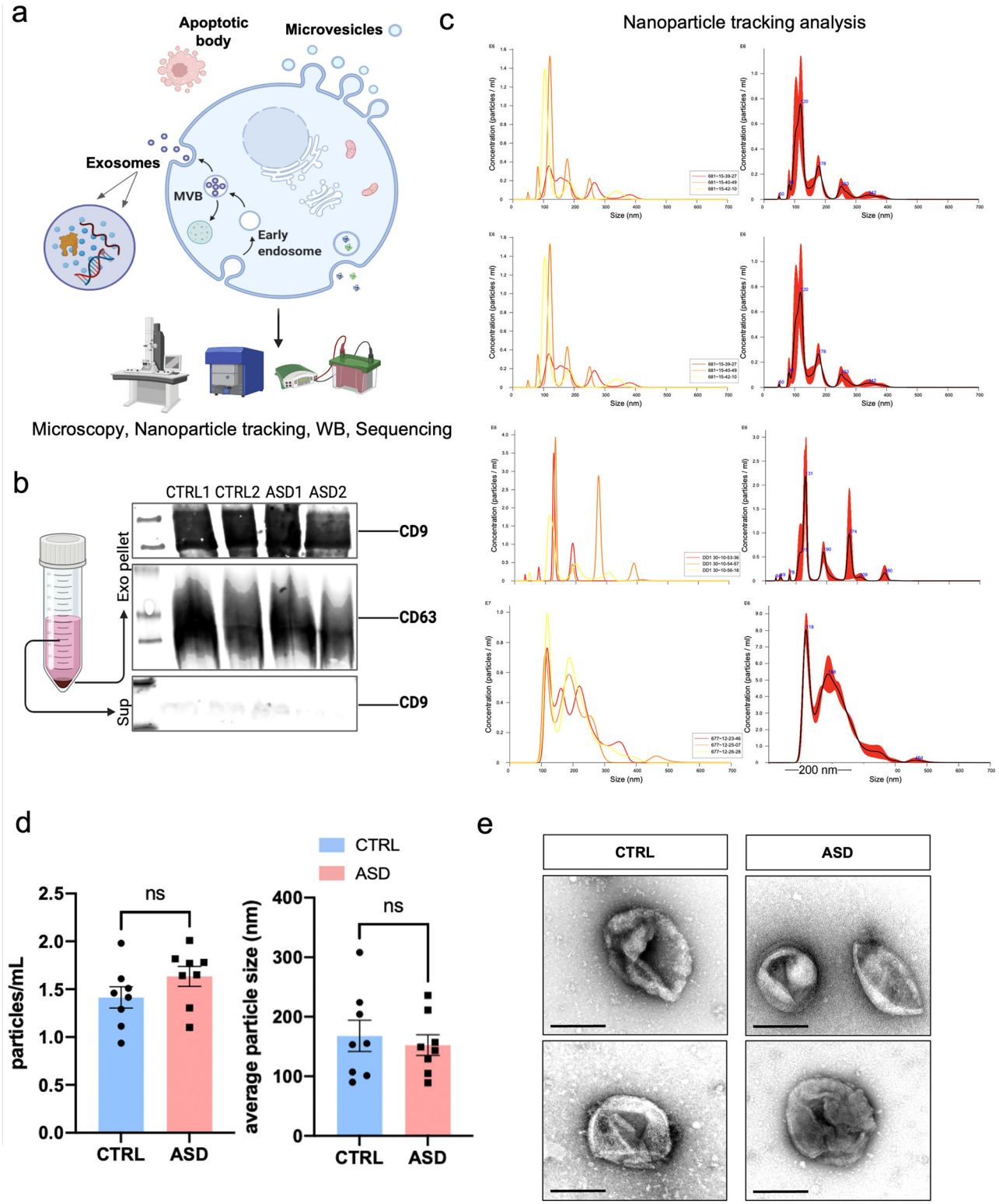

Fig. 2 Exosome abundance in organoid-derived EVs. a Schematic of exosome validation methods. EVs were isolated from maintenance media of CTRL and ASD dorsal forebrain organoids at 60 DIV using a combination of Exo-isolation kit and centrifugation. EVs were then resuspended in either RIPA or PBS buffers, depending on downstream analysis. **b** Representative Western blot examples in pellet and supernatant samples. Only pellets, not supernatant, were positive for exosome markers (CD9, CD63) indicating high efficiency in EV isolation. **c** Representative graphs of nanoparticle tracking analysis (NTA). The x-axis represents concentration (particles/mL), and the y-axis represents particle size (nm). The top four are representative plots from CTRL lines while the bottom four plots are representative examples from ASD lines. The peaks typically appeared in the < 200 nm range, representative of exosome size. **d** Bar graphs depicting no significant difference in either average particle size or concentration between CTRL and ASD EVs at the NTA analysis (Student's t-test). Each point on the graph represents an independent cell line. Data are represented as mean ± SEM. **e** Representative TEM images of EVs isolated from CTRL and ASD organoid media. Vesicles typically displayed a canonical exosome cup/rose shape and size. Scale bar = 200 nm.

RNAs as well as long RNAs both in CTRL and ASD EVs (Fig. 3a). Given the heterogeneity of ASD, no RNAs were commonly altered across all ASD lines. However, several RNAs showed recurrent alterations across multiple ASD lines when compared to CTRL lines. We collectively identified 177 RNAs that were differentially regulated in ASD EVs compared to CTRL EVs. Of those 177 RNAs, 113 were protein-coding, with 58 upregulated and 55 down-regulated. The remaining 64 differentially regulated RNAs were comprised of miRNAs, lincRNAs, snoRNAs, pseudogenes, and some uncharacterized transcripts (Fig. 3b, c). The top 20 differentially regulated protein-coding RNAs in ASD are also shown (Fig. S2c). To gain more insight into the function of

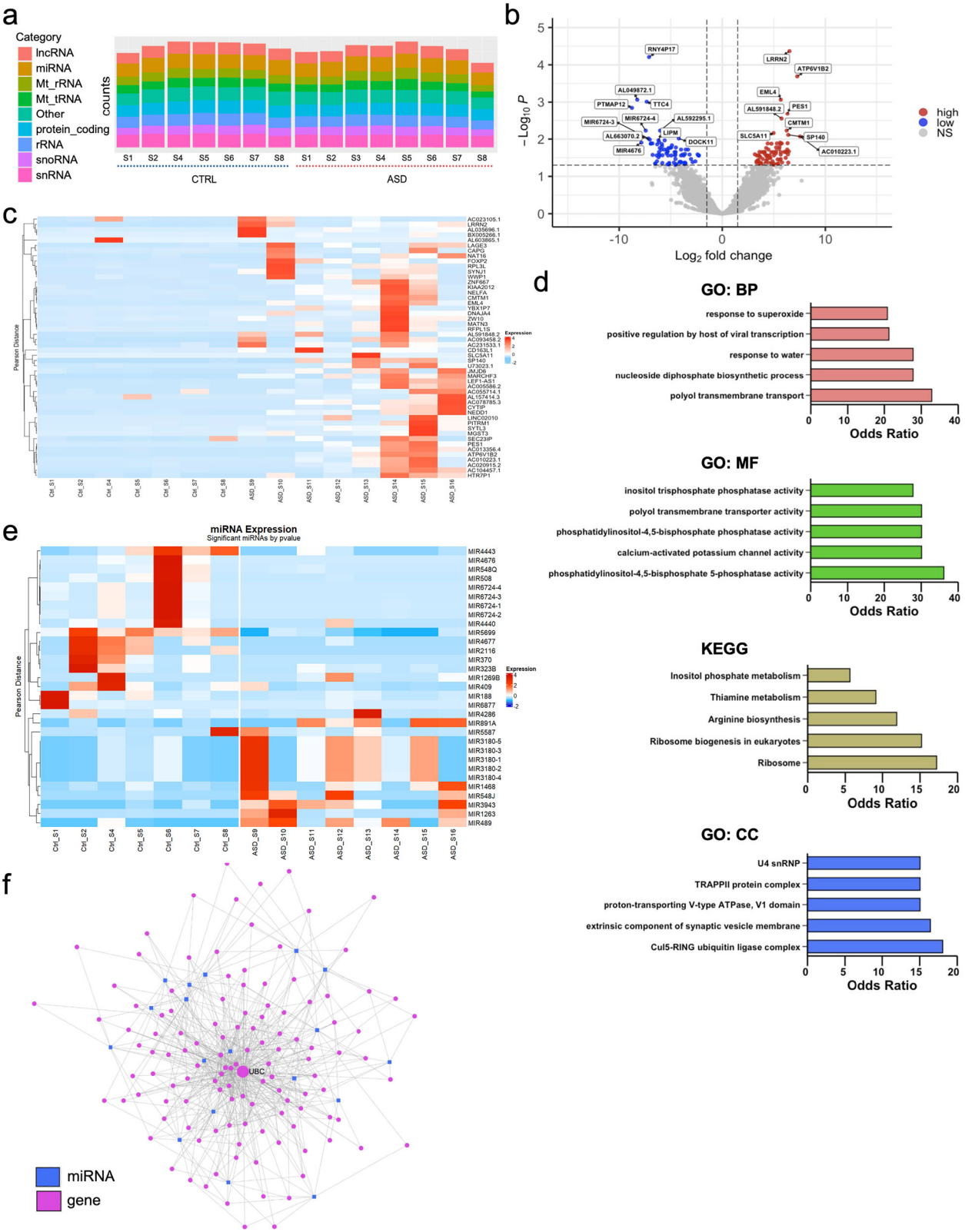

Fig. 3 Differentially regulated RNAs point to translational control and ubiquitin activity in ASD EVs. a RNA counts by category per ASD and CTRL sample (n = 16 samples). CTRL samples CS1 and CS6 are 2 CTRL lines of female origin, while all the other CTRL lines are of male origin. **b** Volcano plot displaying significantly expressed genes. Thresholds of significance used included Log2 FC > +/− 1.5 and adjusted log10 Benjamini-Hochberg corrected $p < +/- 0.05$. **c** Hierarchical and K-means heatmap of the top 50 differentially expressed RNAs in each sample (see supplementary materials for the full list of differentially regulated RNAs). **d** Bar graph of GSEA enrichment terms from the respective pathway database. Terms ordered by descending odds ratio. Significant GSEA categories include i) Gene Ontology: Biological Processes (BP), ii) KEGG Kyoto Encyclopedia of Genes and Genomes, iii) Gene Ontology: Molecular Function (MF), iv) Gene Ontology: Cellular Component (CC). **e** Hierarchical and K-means heatmap of the top 31 differentially expressed miRNAs in each sample; $p < 0.05$. **f** miRNA–gene interaction network and hub gene analysis. Node size corresponds to the degree of connectivity, with larger nodes indicating higher numbers of interactions.

differentially regulated RNAs, we grouped them based on their associated biological process, molecular functions, cellular components, and pathways (Fig. 3d). Molecular function analysis predicted PIP2 phosphatase activity as the most differentially regulated molecular pathway. Among the 177 differentially regulated RNAs, ubiquitin ligase complex and synaptic vesicle membranes were the most enriched cellular components. In the differentially regulated non-coding RNA pool (64 RNAs), there were 31 miRNAs significant at the raw p-value level (Fig. 3e). While some of these miRNAs were previously shown to be EV transported [63–65], most of the differentially regulated miRNAs were novel as EV cargo (Fig. S2d). To predict the functional impact of varied miRNA profiles in EVs across all ASD lines, we performed a miRNA–target gene network topology analysis. The network revealed a highly interconnected regulatory architecture, with several hub genes targeted by multiple EV-enriched miRNAs (Fig. 3f). Ubiquitin C (UBC) emerged as the most central node (degree = 99, betweenness = 4835.98), suggesting a pivotal role in EV-mediated signaling. Other top-ranking genes included heat shock proteins (HSP90AA1, HSP90AB1), transcription factors (TP53, HNF4A), and synaptic regulators (AKT1, CTNNB1). These hubs are implicated in stress response, proteostasis, chromatin remodeling, and synaptic plasticity—processes increasingly recognized as dysregulated in ASD. Our findings reveal that human forebrain organoid-derived EVs carry various RNA subtypes and that RNA content of ASD EVs is vastly different than CTRL EVs.

To compare protein profiles of EVs secreted from CTRL organoids and ASD organoids, we employed label-free mass spectrometry and successfully captured a large pool of proteins from all 16 lines (Fig. 4a, b) with comparable variability (Fig. 4c). Of note, two ASD lines showed lower protein capture than average. Similar to the RNA analysis, we did not find proteins that were commonly altered across all ASD samples. Collectively, 362 proteins were differentially regulated in ASD EVs in comparison to CTRL EVs with the majority exhibiting downregulation (279 downregulated and 83 upregulated) (Fig. 4b, d). We grouped the differentially regulated proteins based on biological process, molecular function, cellular component, and pathway represented (Fig. 4e). The gene ontology (GO) analysis predicted cytoplasmic translation and mRNA stabilization as the most altered biological processes. While molecular function analysis determined ubiquitin ligase and ubiquitin transferase inhibitor activity as the most differentially regulated molecular pathways, the top categories included ribosomal subunits and the B-WICH chromatin remodeling complex in cellular compartment analysis.

To determine if varied molecule expression in EVs across all ASD lines converge upon known biological pathways, we performed topology-based enrichment network analysis (Fig. 5). For RNA cargo, enriched gene clusters were predominantly associated with apoptosis, metabolic regulation, and vesicular trafficking—highlighted by categories such as “intrinsic apoptotic signaling,” “GDP biosynthesis,” and “clathrin-coated endocytosis”. These findings suggest that ASD EVs may influence recipient cells by modulating survival pathways and intracellular transport. In parallel, analysis of differentially expressed proteins revealed a striking convergence on pathways related to translation and RNA processing. Highly enriched terms included “cytoplasmic translation”, “RNA processing”, “peptide metabolic process”, and “gene expression”, underscoring a coordinated disruption in protein synthesis machinery in ASD EVs.

Differentially regulated molecules include ASD risk genes in ASD organoid-derived EVs

Lastly, we sought to determine whether differentially regulated molecules in ASD EVs include any known ASD risk genes. For this, we used the Simons Foundation Autism Research Initiative (SFARI) gene database, which focuses on genes implicated in ASD susceptibility. SFARI gene comparison pointed to 7 ASD risk genes in the differentially regulated RNA pool (Fig. 6a). At the protein level, we found a significant abundance of differentially regulated SFARI risk genes in ASD EVs compared to CTRL EVs (Fig. 6b). Notably, a majority of these proteins were downregulated in ASD and mostly involved in transcription, DNA damage, and chromatin structure (Fig. 6c). In contrast, upregulated proteins were associated with neuronal excitability and calcium signaling. Collectively, these findings suggest that differential regulation of ASD risk genes in ASD-derived EVs reflects key disruptions in synaptic function, RNA processing, DNA stability, and synaptic integrity.

DISCUSSION

In ASD, neural circuits involved in social interaction, communication, and repetitive behaviors are disrupted, potentially due to imbalances in excitatory and inhibitory neurotransmission and altered connectivity. Development of the neuronal circuit and its function relies on a continuous crosstalk between neurons and non-neuronal cells. In the last decade, EVs have gained attention for their role in facilitating intercellular communication by delivering cargo such as RNA and proteins, which can influence a variety of cellular processes in recipient cells [66–71]. The cargo within EVs is dynamic and can vary depending on the cell type of origin, suggesting that EVs may play a central role in modulating neurodevelopmental processes. While recent studies implicate EVs in neuronal phenotypes seen in ASD models with potential use of exosomes as a novel therapeutic tool, the pathology of EVs and its exact impact on the initial insults of the disorder are yet to be determined. Our study takes a critical step in understanding this dynamic by providing the first comprehensive characterization of EVs secreted by multicellular brain organoids derived from both ASD patients and neurotypical controls. By profiling the RNA and proteomic cargo of patient-derived EVs during neurodevelopment, we postulate how EV-mediated intercellular communication may be altered in ASD.

Adopting a protocol for the generation of human dorsal forebrain organoids [59], we generated hundreds of reproducible organoids across 16 different iPSC donors, 8 of which were derived from individuals with idiopathic ASD (Fig. 1, see also Supp Table). The morphological phenotype in ASD-derived brain organoids, specifically the increased size, align with well-documented neurodevelopmental phenotypes observed both in in vitro organoid models of ASD and some patients [72, 73]. This

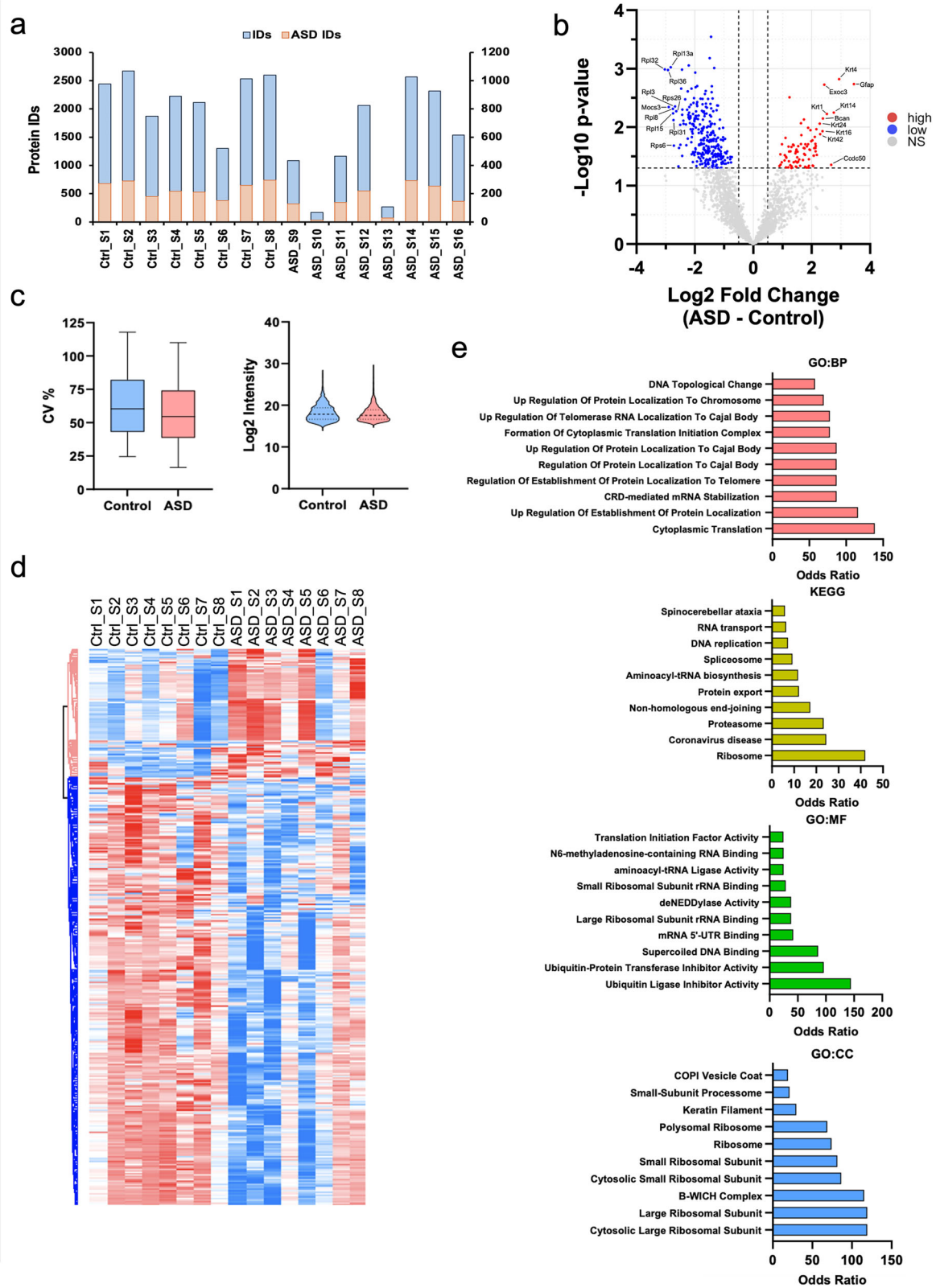

Fig. 4 Altered protein expression comprises translation and protein degradation related categories in ASD EVs. a Protein counts by category per ASD and CTRL sample (n = 16 samples). CTRL samples CS1 and CS6 are 2 CTRL lines of female origin, while all the other CTRL lines are of male origin. **b** Volcano plot displaying proteins expressed significantly. Thresholds of significance used included Log2 FC > +/− 1.5 and adjusted log10 Benjamini-Hochberg corrected $p < 0.05$. **c** Coefficient of variance in CV and ASD lines, (n = 16 samples), non-significant. **d** Clustered heatmap of 362 significant proteins based on a student's t-test analysis ($p < 0.05$). Values based on z-score normalization. **e** Gene ontology analysis of significant proteins using enrichR. Top 10 categories selected ($p < 0.05$); odds ratio observed between ASD and CTRLs. Terms ordered by descending odds ratio. Significant GSEA categories include i) Gene Ontology: Biological Processes (BP), ii) KEGG Kyoto Encyclopedia of Genes and Genomes, iii) Gene Ontology: Molecular Function (MF), iv) Gene Ontology: Cellular Component (CC).

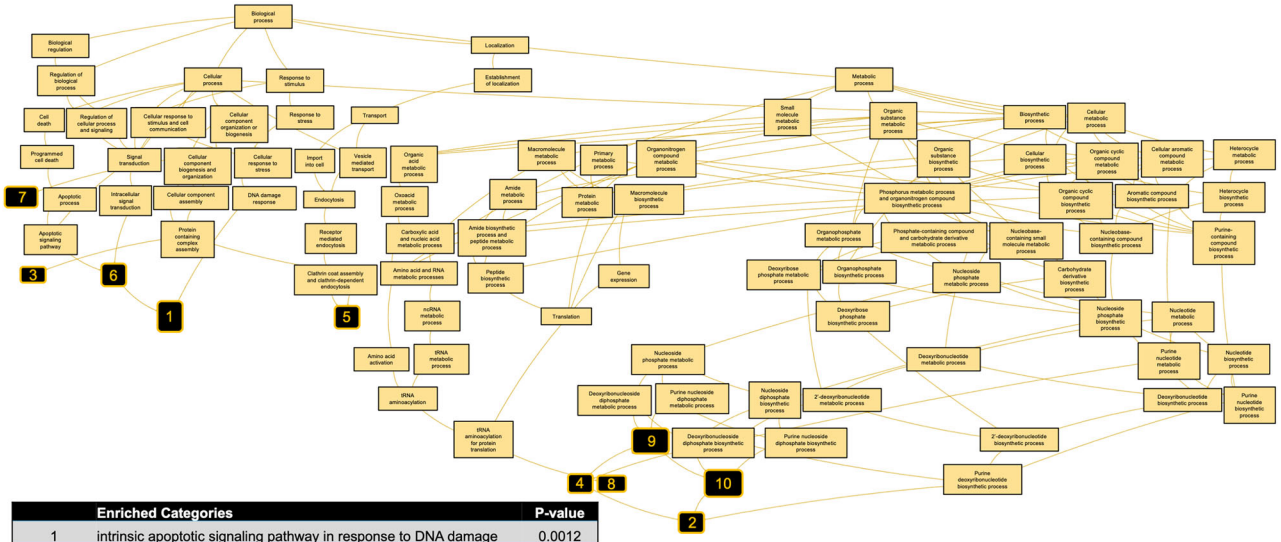

	Enriched Categories	P-value
1	intrinsic apoptotic signaling pathway in response to DNA damage	0.0012
2	dADP biosynthetic process	0.0028
3	SCF complex assembly	0.0028
4	dADP metabolic process	0.0028
5	clathrin coat assembly involved in endocytosis	0.0028
6	intrinsic apoptotic signaling pathway	0.0029
7	ribonucleoprotein complex biogenesis	0.0051
8	glutamyl-tRNA aminoacylation	0.0056
9	purine deoxyribonucleoside diphosphate metabolic process	0.0056
10	purine deoxyribonucleoside diphosphate biosynthetic process	0.0056

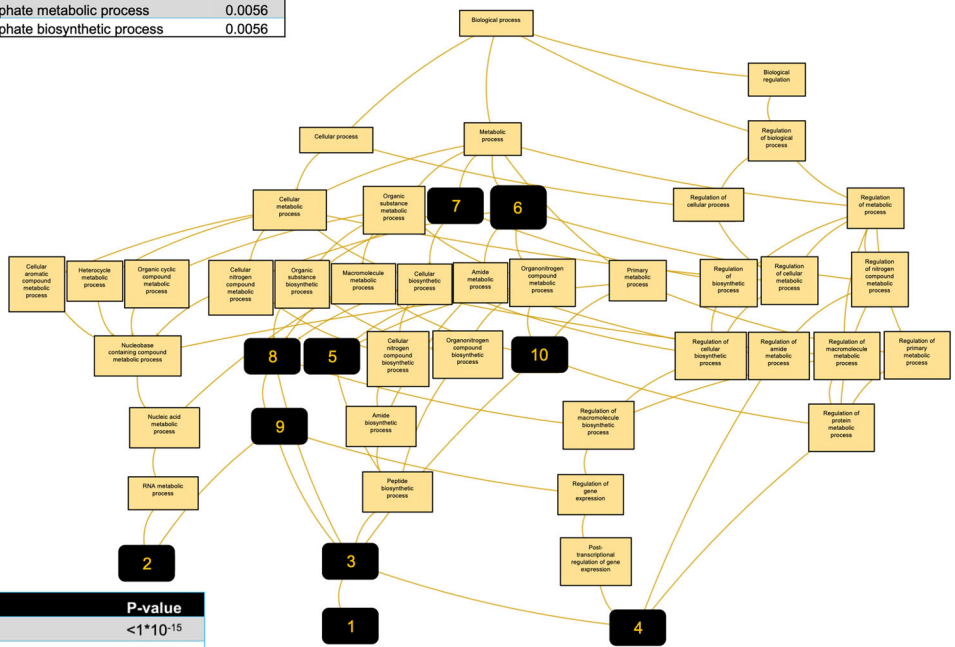

	Enriched Categories	P-value
1	cytoplasmic translation	$<1*10^{-15}$
2	RNA processing	$<1*10^{-15}$
3	translation	$<1*10^{-15}$
4	regulation of translation	$<1*10^{-15}$
5	peptide metabolic process	$<1*10^{-15}$
6	nitrogen compound metabolic process	$<1*10^{-15}$
7	biosynthetic process	$<1*10^{-15}$
8	macromolecule biosynthetic process	$<1*10^{-15}$
9	gene expression	$<1*10^{-15}$
10	protein metabolic process	$<1*10^{-15}$

Fig. 5 Altered pathways predicted by network analysis in ASD EVs. Topology-based network enrichment analysis of differentially expressed genes and proteins in ASD-derived EVs. Top: Gene network analysis revealed 10 significantly enriched categories, including apoptosis, GDP metabolism, and clathrin-mediated endocytosis ($p < 0.01$). Bottom: Protein network analysis identified highly interconnected enrichment in translation, RNA processing, and biosynthetic pathways ($p < 1\times10^{-15}$). Node size reflects the degree of connectivity within the GO network.

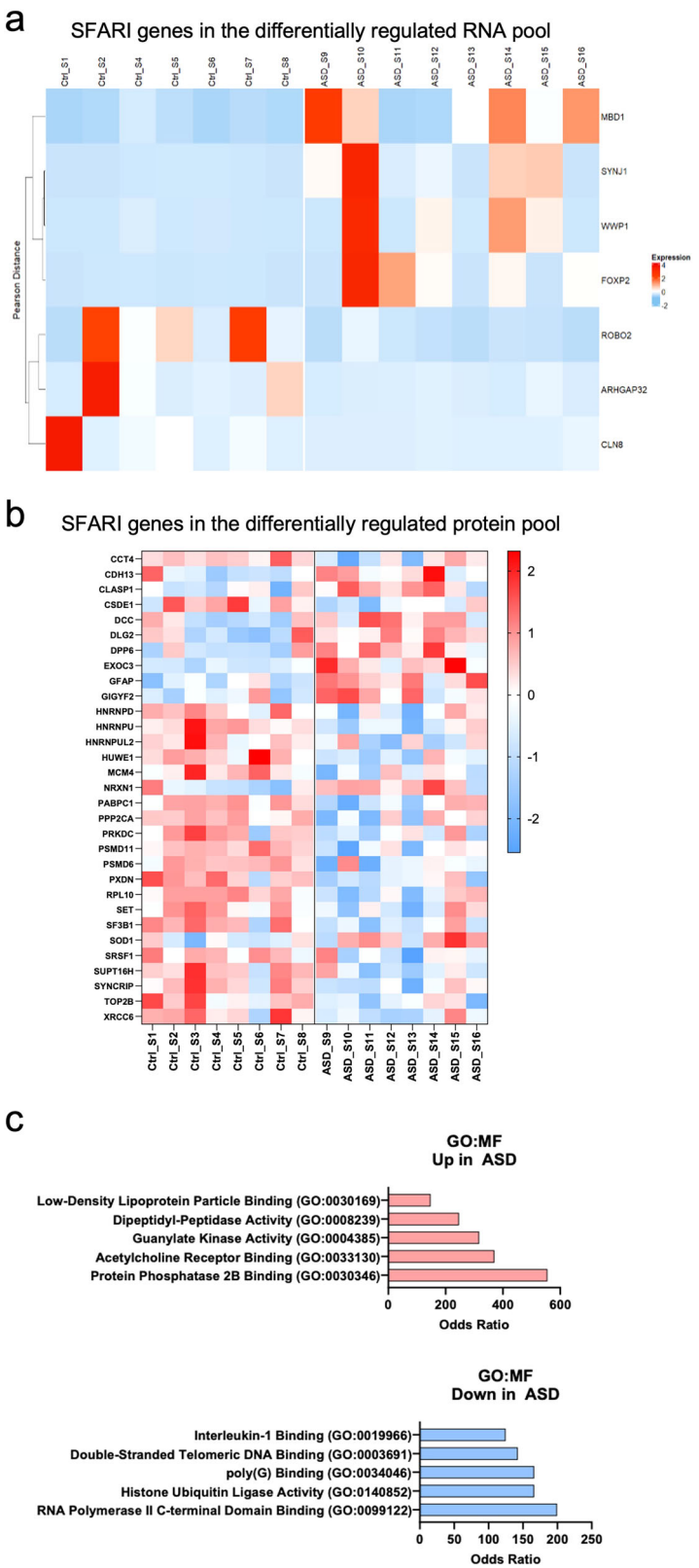

Fig. 6 Differentially regulated RNAs and proteins in ASD EVs include ASD risk genes. a Heatmap of the significant SFARI genes among the differentially expressed mRNAs in each group. Values based on z-score normalization ($p < 0.05$). **b** Heatmap of the significant SFARI genes among the differentially expressed proteins. Values based on z-score normalization ($p < 0.05$). **c** enrichR gene ontology analysis of the significant SFARI risk genes among the differentially expressed proteins in ASD EVs. Top categories selected ($p < 0.05$); odds ratio observed between ASD and CTRL.

phenotype is consistent with the increased brain volume seen in a fraction of ASD patients, particularly during early childhood [74], supporting that brain organoid models could serve as a relevant representation of the abnormal developmental trajectories observed in ASD. The increased thickness of the ventricular zone in ASD organoids further supports this, as it aligns with similar findings reported by other groups in ASD organoids [75] and in patients, where abnormal changes in the subependymal zone have been linked to neurodevelopmental delays and irregular brain development [74]. Despite the genetic variability in iPSC lines, our model system consistently recapitulates key aspects of early brain pathology in neurodevelopmental disorders [54–58]. This reinforces the potential of brain organoids as a platform for studying ASD and exploring therapeutic avenues for modulating early neurodevelopmental disruptions.

Here, we demonstrate the successful isolation of EVs from CTRL and ASD forebrain organoids using kit-based precipitation of EVs. Although recent studies have isolated EVs from CTRL organoids using varying protocols [76, 77] standardized methods for EV isolation remain elusive. Several isolation techniques are employed, such as ultracentrifugation and precipitation-based kits, each with its own advantages and applications [78–81]. Given the limited culture size and heterogeneity of our iPSC lines, we opted for kit-based precipitation to maximize EV yield. We confirmed successful isolation of EVs by 3 different methods-NTA, TEM and Western blotting, ensuring consistent EV isolation across all lines. While we observed no major morphological differences in EVs between ASD and CTRL organoids, the overlap in size and surface markers between exosomes and other microvesicles made it challenging to distinguish specific EV subtypes with certainty. Thus, for the scope of this study, we focused on a deeper analysis of the RNA and proteomic cargo itself, rather than outer differences of EVs, aiming to uncover potential molecular differences in ASD. In our analysis of the RNA cargo in EVs, we observed significant differences both in coding and non-coding RNA content between ASD and CTRL samples (Fig. 3). Although most of the EV studies focus on miRNA content, EVs were also shown to carry mRNAs [82]. In fact, we found that 58 coding RNAs were upregulated and 55 coding RNAs were downregulated in ASD EVs compared to CTRLs (Fig. 3c). While there was no specific coding RNA commonly altered across all ASD samples, some transcripts, such as *FOXP2*, *SP140*, and *MARCHF3* exhibited upregulation in more than 50% of ASD samples compared to all CTRL samples. Intriguingly, these genes have commonly been implicated in the regulation of gene expression. While *FOXP2* is a transcription factor, *SP140* influences chromatin accessibility to regulate expression of genes involved in neuronal development. Similarly, *MARCHF3* functions as an E3 ubiquitin ligase, inducing protein degradation, and thereby regulating protein expression. These alterations are also reflected in our enrichment analysis (see below). Biological process analysis of DEGs also pointed to clinically significant pathways such as polyols and phosphoinositide metabolism (Fig. 3d). Recent findings have suggested that reducing polyol consumption can alleviate gastrointestinal and behavioral symptoms in ASD individuals [83]. Similarly, phosphoinositides, particularly phosphatidylinositol 4,5-bisphosphate (PIP2) and its metabolites, play an important role in regulating cellular signaling pathways involved in neuronal development, synaptic plasticity, and neurotransmitter release [84, 85]. Disruptions in phosphoinositide signaling could affect neuronal connectivity and synaptic function, both of which are central to the pathophysiology of ASD. In addition to coding genes, we also identified a range of upregulated noncoding RNA elements, particularly miRNAs, in ASD-derived EVs (Fig. 3e, Fig. S2d). Specifically, exosomal miRNAs were shown to play a pivotal role in regulating gene expression by modulating mRNA stability and translation [86–88]. miRNA370 was commonly downregulated in all ASD lines compared to the majority of CTRL lines. miRNA370 was previously shown to increase permeability of the BBB [88]. Indeed, altered BBB permeability and associated inflammation have been observed in ASD [89]. On the contrary, miR3943 was upregulated in 6 out of 8 ASD samples compared to all CTRL samples. Intriguingly, this human-specific microRNA has been implicated in the regulation of excitatory synaptogenesis timing [90]. Our study also identified novel miRNAs in the context of EV cargo such as *miRNA6724–1*, *miRNA6724–2*, *miRNA6724–3*, and *miRNA6724–4*. Of note, *miRNA4286* overexpression was identified as an unfavorable prognostic marker in non-small cell lung cancer [91].

We also detected altered expressions of proteins involved in key cellular processes such as ubiquitination, translation, and ribosome biogenesis in ASD EVs (Fig. 4). Perturbations in the ubiquitin-proteasome system, a critical pathway for protein turnover and the degradation of damaged or misfolded proteins, can lead to the accumulation of faulty proteins, triggering neuroinflammatory responses. This disruption is particularly relevant in the context of ASD, where chronic inflammation and immune dysregulation are increasingly recognized as contributing factors to neurodevelopmental impairments [92–94]. Several lines of evidence suggest that alterations in the ubiquitin-proteasome system and other ubiquitin-related pathways may contribute to the onset or severity of ASD [95–100]. Of note, proteins of the B-WICH complex, a regulator of chromatin remodeling [101–103], along with proteins involved in translation and ribosome regulation, compromised the top categories in GO analysis of altered EV proteome in ASD. In fact, whole exome sequencing studies employing large patient cohorts have revealed that the majority of ASD risk genes are chromatin and gene expression regulators [104]. Similarly, altered translation has been implicated in various diverse types of ASD models [105–107]. Most importantly, our topology-based enrichment network analysis of varied molecule expression found in EVs across patient lines pointed to limited biological pathways most of which have been linked to ASD (Fig. 5). For RNA cargo, enriched gene clusters were predominantly associated with apoptosis, metabolic regulation, and vesicular trafficking, as observed by top categories in the topology map (GDP biosynthesis, clathrin-endocytosis, apoptotic signaling). These findings suggest that ASD EVs may influence recipient cells by modulating cell survival pathways and intracellular transport. The network analysis of proteins with varied expressions across ASD EVs found enrichment in translational and gene expression regulation categories. This network analysis aligns with the findings from the GO analyses of differentially regulated EV proteins from individual lines, which collectively pointed to gene regulation pathways (Fig. 4). Taken together, these findings suggest that the most in ASD EVs are linked to both EV formation and transport (endocytotic), and regulation of translational control in recipient cells (translational regulation, ribosomal enrichments). Our findings support the hypothesis that dysregulation of translational control is a converging mechanism, not only in syndromic, but also in idiopathic forms of ASD [107].

Lastly, among the differentially regulated coding RNAs and proteins in ASD-derived EVs, several SFARI-based ASD risk genes were identified. Notably, the RNA of FOXP2, a transcription factor implicated in neurodevelopment and speech disorders [108], was differentially regulated- upregulated in some ASD EV lines and downregulated in others. Similarly, the RNA of the epigenetic regulator MBD1, whose deficiency is linked to autism-related behaviors in mice [109], was also among the altered ASD risk genes. MBD1 was upregulated in the majority of ASD lines compared to the majority of CTRL lines. In contrast, RNAs of certain ASD risk genes that were downregulated in ASD EVs are linked to axon guidance (i.e., ROBO2). Similarly, the CLASP1 protein, linked to cell polarization and axon guidance, was upregulated in EVs from the majority of ASD lines compared to CTRL EVs. However, most of differentially expressed EV proteins that are recognized as ASD risk genes were downregulated in ASD

EVs. These proteins are primarily involved in RNA splicing, RNA processing, and protein synthesis. Together, these categories represented 75% of the downregulated ASD risk genes in the ASD EV proteome, further supporting the hypothesis that dysregulation of translational control is a converging mechanism in ASD.

Limitations and Future Directions

While our study provides important insights into the differential cargo of EVs in ASD-derived organoids, several limitations must be acknowledged. One limitation is that the field of EV studies is at its early stages, and the lack of standardized protocols for the isolation and characterization of EVs from multicellular tissues presents a challenge. Currently, both ultracentrifugation and precipitation methods are employed for EV isolation, yet no consensus exists on the optimal approach for isolating EVs from complex models such as organoids. In this study, we opted for precipitation to maximize the yield of EVs from a broad range of lines. While ultracentrifugation could provide a purer EV population, the significant scaling required for organoid cultures would not justify the marginal benefits for our study's scope. Future studies should compare these two isolation methods directly to establish clear guidelines for EV research in brain organoid models. Another limitation concerns the characterization of the isolated EVs. Despite using an "exosome-specific" precipitation kit, the vesicles obtained exhibited overlapping size distributions between exosomes and microvesicles, as determined by nanoparticle tracking analysis (NTA). As a result, it was not possible to conclusively separate exosomes from microvesicles, or to determine whether the isolated population consisted of pure exosomes, microvesicles, or aggregates of smaller exosomes. Therefore, we refer to these vesicles as "extracellular vesicles (EVs)" throughout this study, despite compelling evidence to suggest that they primarily represent exosomes.

ASD exhibits a significant male bias in prevalence, with males diagnosed approximately four times more than females. The differences in symptom presentation may contribute to females being underdiagnosed or receiving diagnoses later than males. Current diagnostic tools, primarily developed based on male-centric data, may not adequately capture the female autism-related phenotype. This highlights the need for more nuanced research to understand the complexities of sex differences in ASD. Because understanding sex differences in ASD is crucial for developing personalized medicine approaches. In the present study, we first wanted to establish whether there is EV pathology in ASD human-derived models, which enables capturing very early neurodevelopmental signatures. Our study is not powered to explore sex differences (8/8 of our ASD lines and 6/8 of our CTRL are of male origin). As such, an interesting future direction would be to investigate sex differences in EV pathology using larger cohorts and similar organoid-based models. Given the strong male bias in ASD diagnosis and differences in symptom presentation between sexes, such studies could shed light on sex-specific mechanisms which can allow for the development of more personalized diagnostic approaches. Additionally, although our sample size was sufficient to detect early differences in EV cargo, it was not designed to identify robust biomarkers for ASD. Future research with larger, more diverse cohorts could explore whether specific RNA or protein expression signatures in EVs might serve as reliable, non-invasive approaches for early ASD diagnosis and monitoring of neurodevelopmental conditions. Related to sample size, heterogeneity of ASD also poses a significant challenge in research, as it reflects diverse etiologies and outcomes within the spectrum. This variability complicates our efforts to identify cellular mechanisms, develop effective interventions, and predict individual trajectories. Like most other studies, our work is also on a relatively small sample size, limiting the generalizability of findings to the broader ASD population. However, by focusing on specific developmental time points and a specific cellular process, it provides unique insights and contributions to generating novel hypotheses in ASD research. It has also been established that the causes of ASD are complex and involve a combination of genetic and environmental factors, with varying contributions in different individuals. Our study was designed to determine inherent deficits in EVs derived from ASD patient iPSCs, independent of environmental factors. An interesting future extension would be to investigate how environmental exposures alter EV densities and content in control models and in models with pre-genetic predispositions for ASD.

Brain organoids recapitulate key aspects of early brain development providing a platform to investigate the molecular and cellular mechanisms underlying neurodevelopmental disorders. When derived from patient iPSCs, they can offer potentially more accurate understanding of disease pathogenesis. This also allows to model individual variations in disease presentation and response to treatment. Although cortical organoids offer a valuable model for studying early neurodevelopmental processes, they do not fully recapitulate the functional and structural complexity of the mature brain. Consequently, the findings from this study are best understood in the context of early brain development. To better understand the translational relevance of our findings, it will be important to validate these results in in vivo models, such as mouse-organoid xenografts. Finally, while our study demonstrates significant differences in EV cargo between ASD and CTRL organoids, the functional implications of these differences remain speculative. Future work should focus on the specific biological effects of EV-mediated signaling, particularly how the altered cargo influences critical pathways such as protein synthesis, RNA splicing, and synaptic function. By employing more targeted functional assays, it will be possible to determine the precise role of EVs in modulating ASD-related neurodevelopmental processes and to explore their potential as biomarkers or therapeutic targets.

CONCLUSIONS

Our study, for the first time, reports a comparative analysis between EVs in human brain organoids derived from healthy controls and from individuals with ASD. EVs are recognized as regulators of brain development by facilitating cell-to-cell communication, and influencing processes like neurogenesis, synaptogenesis, and myelination, potentially playing a role in neurodevelopmental disorders. We identified significant alterations in RNA and protein content in ASD EVs at relatively earlier time points of brain organoid development. Gene ontology and network analysis pointed to RNA regulation, translation, DNA damage, and chromatin regulation, suggesting that EV pathology in ASD may contribute to impaired gene expression regulation, a hallmark of neurodevelopmental disorders. While most of these processes have been linked to ASD pathology and etiology, our study identifies EV pathology and EV-mediated non-cell-autonomous regulation of brain development as a potential factor in ASD etiology. Understanding non-cell-autonomous regulation of neuronal activity in ASD is crucial in addressing the underlying mechanisms of the disorder and for developing targeted therapies. Our findings not only advance our understanding of the role of EVs in ASD mechanisms but also sets the stage for exploring their potential as biomarkers, or therapeutic targets, in the treatment of ASD.

MATERIALS AND METHODS

iPSC Lines

iPSC lines were purchased from NIH, CIRM repositories and Coriell Institute (Supplementary Table 1). Each repository characterized and validated cells as pluripotent and performed karyotyping to ensure the genomic integrity of each reprogrammed line. ASD lines MH0148698 and MH0148713 from a

NIMH collection were genetically characterized and published [110]. A total of 16 different iPSC lines (8 CTRL, 8 ASD) were utilized. All ASD samples were derived from non-syndromic cases and were not associated with any known genetic anomaly (see also Supplementary Table). All ASD iPSC lines were derived from males. To maintain consistency and based on availability, we also used CTRL lines that were derived from males except two lines. All iPSC lines were maintained on Vitronectin-coated plates and fed with Essential 8 (E8) + E8 supplement (ThermoFisher, CAT#: A1517001). All iPSC lines were cultured simultaneously to control for idiosyncratic culturing conditions. In all experiments, low passages (less than 18) were used, and all differentiations were derived from a single clone for each line.

Dorsal forebrain organoid generation

Cerebral organoids were generated using a modified version of a previously published protocol [59]. Briefly, on day 0, cultured human iPSCs, 80–90% confluent, were dissociated to single cells with Accutase (Gibco), and 9000 cells per well were reaggregated in ultra-low cell-adhesion 96-well plates in Cortical Differentiation Medium (CDM) I, containing Glasgow-MEM (Gibco), 20% Knockout Serum Replacement (Gibco), 0.1 mM Minimum Essential Medium non-essential amino acids (MEM-NEAA) (Gibco), 1 mM pyruvate (Gibco), 0.1 mM 2-mercaptoethanol (Gibco), 100 U/mL penicillin, and 100 µg/mL streptomycin (Corning). From day 0–day 3, ROCK inhibitor Y–27632 (Millipore) was added to the media at a final concentration of 20 µM. From day 0–day 10, Wnt inhibitor IWR1 (Calbiochem) and TGFβ inhibitor SB431542 (Stem Cell Technologies) were added at a concentration of 3 µM and 5 µM, respectively. From day 10, the floating aggregates were cultured in ultra-low attachment culture dishes (Corning) under orbital agitation (50 rpm) in CDM II, containing DMEM/F12 medium (Gibco), 2 mM Glutamax (Gibco), 1% N2 (Gibco), 1% Chemically Defined Lipid Concentrate (Gibco), 0.25 µg/mL fungizone (Gibco), 100 U/mL penicillin, and 100 µg/mL streptomycin. On day 18 cell aggregates were transferred to CDM III, consisting of CDM II supplemented with 10% fetal bovine serum (FBS) (GE-Healthcare), 5 µg/mL heparin (Sigma), and 1% Matrigel (Corning) and maintained at 50 rpm. From day 24 until day 50, organoids were cultured in CDM IV, consisting of CDM III supplemented with B27 supplement (Gibco) and 2% Matrigel.

Confocal microscopy

To prepare organoids for immunohistochemistry, they were drop-fixed in 4% paraformaldehyde, dehydrated in 30% sucrose and embedded in Tissue-Tek using OCT compound (CAT#: 4583) and biopsy molds. Organoids were then serially cryosectioned onto slides at 30 µm. Thus, each slide from this sectioning contained 3–4 unique sections/Fields of View (FOV) per each organoid studied. Using this approach, we were able to robustly assess both independent and focal cell populations in each biological and technical organoid replicate. In further preparation, all sections underwent heat-mediated antigen retrieval in the citrate buffer and primary antibodies were incubated for each section overnight. Primary antibodies used were SOX2 (1:500, Abcam, ab92494), Beta-III-tubulin (1:500, Abcam, ab78078), Ki67 (1:250, ThermoFisher, CAT#: MA5-14520), PHC3 (1:200, ThermoFisher, CAT#: H00080012-B01P). Secondary antibodies were incubated for 2 h at room temperature and comprised antibodies for rabbit (Fluor 488 CAT#: A11008 & Fluor 633 CAT#: A21070), mouse (Fluor 488 CAT#: A11001 & Fluor 633 CAT#: A21052) and were used at a 1:2000 dilution and sourced from Life Technologies. Microscopy was completed on an Olympus IX81 Laser-Scanning Confocal Microscope, controlled by proprietary Olympus FluoView software. Images were typically acquired at 1200 × 1200-pixel resolution with optical *Z* slices (step sizes) ranging from 1–10 µm depending on the unit of analysis. All 16 lines were used for immunofluorescence quantifications.

EV isolation

EVs were isolated from organoid media at 60 DIV. 10 days prior to media collection, the organoid media was changed to FBS-depleted CDM IV. CDM IV media was ultra-centrifuged at 100,000 g overnight to remove FBS-derived vesicles. This ensures that the media collected at 60 DIV contains EVs derived solely from organoids. Cells were maintained in FBS-depleted CDM IV and at day 60 media was collected and processed using the Total Exosome Isolation Reagent (ThermoFisher CAT#: 4478359). Briefly, 10 mL of media was mixed with 5 mL of total exosome reagent and incubated at 4 C overnight. The next day, samples were centrifuged at 10,000 g for 1 h and the pellet was resuspended in 1x PBS or RIPA buffer, depending on the downstream analysis. Samples resuspended in 1X PBS were used for RNA sequencing, TEM analysis and NTA while samples resuspended in RIPA buffer were used for proteomics and Western blot.

Western blot

For Western blot, EVs were lysed using RIPA buffer and sonication. 30 µg of total protein of each sample was separated on 10% SDS-PAGE under non-reducing conditions and transferred onto a nitrocellulose membrane (BioRad CAT#: 1620113). The membranes were blocked overnight with 5% milk at 4 °C and incubated with primary antibodies (ABs) against CD63 (1:500, ThermoFisher, CAT#: 10628D) and CD9 (1:500, ThermoFisher, CAT#: MA5-31980) for 2 h at RT. After washing, the blots were incubated with HRP-conjugated anti-mouse and anti-rabbit IgG secondary antibody (1:2000, IRDye® 680RD, CAT#: 926-68070 & IRDye® 800CW CAT#: 926-32210, Licor) for 1 h at RT. Protein expression was visualized using the Licor Odyssey® M Imaging system.

Transmission electron microscopy imaging

For negative staining TEM analysis, 5 µL of EVs in PBS (0.1 µg/µL) were placed on a glow-discharge formvar and carbon-coated 400 mesh grid and allowed to settle for 1 min. The sample was blotted and negatively stained with 50 µL of aqueous uranyl acetate (1.5%). After 1 min, the grid was blotted and air-dried for 5 min. Grids were imaged using a JEM-1400 transmission electron microscope (JEOL, USA, Inc., Peabody, MA) operated at 100 kV and images were captured on a Veleta 2 × 2 K CCD camera (EM-SIS, Germany).

Nanoparticle tracking analysis

NTA was performed using a previously established protocol [111, 112]. All samples were diluted in PBS to a final volume of 1 ml. Ideal measurement concentrations were found by pre-testing the ideal particle per frame value (20–100 particles/frame). Following settings were set according to the manufacturer's software manual (NanoSight NS500 User Manual, MAN0513-06-EN-00, 2016): camera level was increased until all particles were distinctly visible not exceeding a particle signal saturation over 20%, camera level 11, BLUE405, 1498 frames. Autofocus was adjusted so that indistinct particles were avoided. For each measurement, five 1-min videos were captured under the following conditions: cell temperature: 24 °C; Syringe speed: 40 µl/s. After capture, the videos have been analyzed by the in-build NanoSight Software NTA 3.4 Build 3.4.003 with a detection threshold 5–18.

Small RNA library preparation

Small RNA libraries were generated using NEXTFlex Small RNA Library Prep Kit v4 (Revvity). This kit is designed to capture short RNAs (17–65 nucleotides) with 5′ monophosphorylated and 3′ hydroxylated ends. The kit also allows for the capture of larger molecules (< 200 bp) by using the no size selection protocol. The manufacturer's instructions were followed through PCR amplification including 3′ adenylated adapter ligation, 5′ adapter ligation and RT first strand synthesis. Following PCR amplification, the libraries were cleaned up using the provided magnetic beads and the resulting pellet was resuspended in 11 µL of ultra-pure water. Sample concentrations were quantified using a NanoDrop Spectrophotometer, QC was evaluated using an Agilent Bioanalyzer Sample and ran on a picogel.

RNA sequencing

The small RNAs from exosomes were isolated using the Total Exosome RNA & Protein Isolation Kit (ThermoFisher). Purified small RNA integrity was checked using a small RNA QC kit on 2100 Bioanalyzer (Agilent Technologies, Santa Clara, CA), and the concentration was measured using the Qubit Fluorometer (ThermoFisher Scientific, Inc., CA). Preparation of small RNA sample library and sequencing were performed by the Genomics Resources Core Facility at Weill Cornell Medicine using the NEXTFLEX® Small RNA-Seq Kit v4 with UDIs kit (Revvity Inc.,), according to the manufacturer's instructions. The normalized cDNA libraries were pooled and sequenced on Illumina NovaSeq X Plus sequencer with pair-end 50 cycles. The raw sequencing reads in BCL format were processed through bcl2fastq 2.19 (Illumina) for FASTQ conversion and demultiplexing.

Bioinformatics pipeline for RNA sequencing

Approximately 5–20 million paired-end reads were generated per sample. Sequencing adapters and duplicate sequence reads were removed, and

low-quality reads trimmed using *Trimmomatic* (version 0.39). Cleaned reads were aligned to the reference human genome (version GRCh38.99) using *STAR* alignment (version 2.7.10b). Read counts of genetic features were obtained by the *SubRead* package (version 2.0.3). The *DESeq2* R/Bioconductor package (version 1.44.0) was used to normalize count data and identify the differentially expressed genes (DEGs) between control and ASD samples. Significant differentially expressed genes were defined by a p value < 0.05 and a $\log_2$ fold change > 1.5 as thresholds. A minimum threshold of expression was set at 25%, representing the number of samples with non-zero expression values that would be considered for differential analysis. Employing these parameters, 177 differentially expressed genes and RNA elements were identified. Gene Ontology and pathway analyses were performed using the *clusterProfiler* package (version 4.12.6) in R. Cutoffs of significance were based on p-value and Benjamini-Hochberg (BH) adjusted p-value. All statistical analyses were performed in R (version 4.4.1). Figures were generated using *ggplot2* (version 3.5.1), *DESeq2* (version 1.44.0), *EnhancedVolcano* (version 1.22.0), and *enrichplot* (version 1.24.2).

Sample preparation and label free proteomics

The protein samples were acetone precipitated and re-suspended in 0.1% RapiGest (Waters), 25 mM ammonium bicarbonate. The samples were then reduced with DTT, alkylated with iodoacetamide, and digested overnight with trypsin at 37 °C. The digests were desalted by C18 Stage-tip columns. The digests were analyzed using a Thermo Fisher Scientific EASY-nLC 1200 coupled on-line to a Fusion Lumos mass spectrometer (ThermoFisher Scientific). Buffer A (0.1% FA in water) and buffer B (0.1% FA in 80% ACN) were used as mobile phases for gradient separation. A 75 µm × 15 cm chromatography column (ReproSil-Pur C18-AQ, 3 µm, Dr. Maisch GmbH, Germany) was packed in-house for peptide separation. Peptides were separated with a gradient of 5–40% buffer B over 30 min, 40–100% B over 10 min at a flow rate of 400 nL/min. The Fusion Lumos mass spectrometer was operated in a data independent acquisition (DIA) mode. MS1 scans were collected in the Orbitrap mass analyzer from 350–1400 m/z at 120 K resolutions. The instrument was set to select precursors in 45 × 14 m/z wide windows with 1 m/z overlap from 350–975 m/z for HCD fragmentation. The MS/MS scans were collected in the orbitrap at 15 K resolution. Data were searched against the human Uniprot database (8/7/2021) using DIA-NN v1.8 and filtered for 1% false discovery rate for both protein and peptide identifications

Bioinformatics pipeline for proteomics analysis

Perseus (v2.0.7.0) (PMID: 27348712) was applied for downstream data processing and analysis. Data quality thresholds included protein group quantification at a 40% inclusion rate in at least one group (n = 8). Protein intensities were log2 transformed and normalized through quantile normalization, with missing values imputed from normal distribution (width 0.3, downshift 1.8). Proteins were subjected to PCA and hierarchical clustering using an unpaired student's t-test using Euclidean distance and average linkage clustering ($p < 0.05$). Proteins were Z-score normalized. Gene Ontology (GO) functional enrichment and network/pathway analysis were conducted using gProfiler and enrichR databases for GO biological processes, cellular components, molecular functions, and KEGG pathways. Enrichment analysis was restricted to the top 10 categories with the highest statistically significant odds ratios comparing ASD and control groups ($p < 0.05$; PMID: 31066453, PMID: 27141961). PCA plots and heatmaps were generated in Perseus. Bar and violin plots were created in GraphPad Prism (v10.0.2) or Microsoft Excel. Comparative proteome analysis was conducted using the Simons Foundation Autism Research Initiative (SFARI) online database (PMID: 24090431).

DATA AVAILABILITY

RNA sequencing and proteomics data were deposited in dbGaP and PRIDE (only proteomics).

REFERENCES

1. Ramaswami G, Geschwind DH. Genetics of autism spectrum disorder. Handb Clin Neurol. 2018;147:321–9.
2. Straiton D, Pomales-Ramos A, Broder-Fingert S. Health equity and rising autism prevalence: Future research priorities. Pediatrics. 2024;154:e2023064262. https://doi.org/10.1542/peds.2023-064262.
3. Rylaarsdam L, Guemez-Gamboa A. Genetic causes and modifiers of autism spectrum disorder. Front Cell Neurosci. 2019;13:385 https://doi.org/10.3389/fncel.2019.00385.
4. Gentilini D, Cavagnola R, Possenti I, Calzari L, Ranucci F, Nola M, et al. Epigenetics of autism spectrum disorders: A multi-level analysis combining epi-signature, age acceleration, epigenetic drift, and rare epivariations using public datasets. Curr Neuropharmacol. 2023;21:2362–73. https://doi.org/10.2174/1570159X21666230725142338.
5. Saeliw T, Permpoon T, Iadsee N, Tencomnao T, Hu VW, Sarachana T, et al. LINE-1 and Alu methylation signatures in autism spectrum disorder and their associations with the expression of autism-related genes. Sci Rep. 2022;12:13970. https://doi.org/10.1038/s41598-022-18232-6.
6. Meltzer A, Van de Water J. The role of the immune system in autism spectrum disorder. Neuropsychopharmacology. 2017;42:284–98. https://doi.org/10.1038/npp.2016.158.
7. Hughes HK, Moreno RJ, Ashwood P. Innate immune dysfunction and neuroinflammation in autism spectrum disorder (ASD). Brain, Behav, Immun. 2023;108:245–54. https://doi.org/10.1016/j.bbi.2022.12.001.
8. Ellul P, Maruani A, Vantalon V, Humeau E, Amestoy A, Anchordoqui A, et al. Maternal immune activation during pregnancy is associated with more difficulties in socio-adaptive behaviors in autism spectrum disorder. Sci Rep. 2023;13:17687. https://doi.org/10.1038/s41598-023-45060-z.
9. Dutra ML, Dias P, Freiberger V, Ventura L, Comim CM, Martins DF, et al. Maternal immune activation induces autism-like behavior and reduces brain-derived neurotrophic factor levels in the hippocampus and offspring cortex of C57BL/6 mice. Neurosci Lett. 2023;793:136974. https://doi.org/10.1016/j.neulet.2022.136974.
10. Tartaglione AM, Villani A, Ajmone-Cat MA, Minghetti L, Ricceri L, Pazienza V, et al. Maternal immune activation induces autism-like changes in behavior, neuroinflammatory profile, and gut microbiota in mouse offspring of both sexes. Transl Psychiatry. 2022;12:384. https://doi.org/10.1038/s41398-022-02149-9.
11. Edgar JC. Identifying electrophysiological markers of autism spectrum disorder and schizophrenia against a backdrop of normal brain development. Psychiatry Clin Neurosci. 2020;74:1–11. https://doi.org/10.1111/pcn.12927.
12. Green HL, Shen G, Franzen RE, McNamee M, Berman JI, Mowad TG, et al. Differential maturation of auditory cortex activity in young children with autism and typical development. J Autism Developmental Disord. 2023;53:4076–89. https://doi.org/10.1007/s10803-022-05696-8.
13. Napolitano A, Schiavi S, La Rosa P, Rossi-Espagnet MC, Petrillo S, Bottino F, et al. Sex differences in autism spectrum disorder: Diagnostic, neurobiological, and behavioral features. Front Psychiatry. 2022;13:889636. https://doi.org/10.3389/fpsyt.2022.889636.
14. Maenner MJ, Shaw KA, Bakian AV, Bilder DA, Durkin MS, Esler A, et al. Prevalence and characteristics of autism spectrum disorder among children aged 8 years - autism and developmental disabilities monitoring network, 11 sites, United States, 2018. MMWR Surveill Summ. 2021;70:1–16.
15. Baxter AJ, Brugha TS, Erskine HE, Scheurer RW, Vos T, Scott JG. The epidemiology and global burden of autism spectrum disorders. Psychological Med. 2015;45:601–13. https://doi.org/10.1017/S003329171400172X.
16. Santos CLD, Barreto II, da Silva ACF, Soriano JFB, Castro JLS, Tristão LS, et al. Behavioral therapies for the treatment of autism spectrum disorder: a systematic review. Clinics. 2024;80:100566. https://doi.org/10.1016/j.clinsp.2024.100566.
17. Alessio N, Brigida AL, Peluso G, Antonucci N, Galderisi U, Siniscalco D. Stem cell-derived exosomes in autism spectrum disorder. Int J Environ Res Public Health. 2020;17:944 https://doi.org/10.3390/ijerph17030944.
18. Geschwind DH. Genetics of autism spectrum disorders. Trends Cogn Sci. 2011;15:409–16. https://doi.org/10.1016/j.tics.2011.07.003.
19. Muhle R, Trentacoste SV, Rapin I. The genetics of autism. Pediatrics. 2004;113:e472–e486. https://doi.org/10.1542/peds.113.5.e472.
20. Siniscalco D, Cirillo A, Bradstreet JJ, Antonucci N. Epigenetic findings in autism: new perspectives for therapy. Int J Environ Res Public Health. 2013;10:4261–73. https://doi.org/10.3390/ijerph10104261.
21. Saeedi S, Israel S, Nagy C, Turecki G. The emerging role of exosomes in mental disorders. Transl Psychiatry. 2019;9:122. https://doi.org/10.1038/s41398-019-0482-3.
22. Huo L, Du X, Li X, Liu S, Xu Y. The emerging role of neural cell-derived exosomes in intercellular communication in health and neurodegenerative diseases. Front Neurosci. 2021;15:738442. https://doi.org/10.3389/fnins.2021.738442.
23. Janas AM, Sapoń K, Janas T, Stowell MH, Janas T. Exosomes and other extracellular vesicles in neural cells and neurodegenerative diseases. Biochimica et Biophysica Acta. 2016;1858:1139–51. https://doi.org/10.1016/j.bbamem.2016.02.012.
24. Samanta S, Rajasingh S, Drosos N, Zhou Z, Dawn B, Rajasingh J. Exosomes: New molecular targets of diseases. Acta Pharm Sin. 2017;39:501 https://doi.org/10.1038/aps.2017.17.

25. Lee Y, El Andaloussi S, Wood MJA. Exosomes and microvesicles: Extracellular vesicles for genetic information transfer and gene therapy. Hum Mol Genet. 2012;21:R125–R134. https://doi.org/10.1093/hmg/dds317.
26. Bakhti M, Winter C, Simons M. Inhibition of Myelin Membrane Sheath Formation by Oligodendrocyte-derived Exosome-like Vesicles. J Biol Chem. 2011;286:787–96.
27. Faure J, Lachenal G, Court M, Hirrlinger J, Chatellard-Causse C, Blot B, et al. Exosomes are released by cultured cortical neurons. Mol Cell Neurosci. 2006;31:642–8.
28. Kang DJ, Oh S, Ahn SM, Lee BH, Moon MH. Proteomic analysis of exosomes from human neural stem cells by flow field-flow fractionation and nanoflow liquid chromatography-tandem mass spectrometry. J Proteome Res. 2008;7:3475–80.
29. Kramer-Albers EM, Bretz N, Tenzer S, Winterstein C, Mobius W, Berger H, et al. Oligodendrocytes secrete exosomes containing major myelin and stress-protective proteins: Trophic support for axons?. Proteom Clin Appl. 2007;1:1446–61.
30. Wang SW, Cesca F, Loers G, Schweizer M, Buck F, Benfenati F, et al. Synapsin I is an oligomannose-carrying glycoprotein, acts as an oligomannose-binding lectin, and promotes neurite outgrowth and neuronal survival when released via glia-derived exosomes. J Neurosci. 2011;31:7275–90.
31. Xin HQ, Li Y, Buller B, Katakowski M, Zhang Y, Wang XL, et al. Exosome-mediated transfer of miR-133b from multipotent mesenchymal stromal cells to neural cells contributes to neurite outgrowth. Stem Cell. 2012;30:1556–64.
32. Yuyama K, Sun H, Mitsutake S, Igarashi Y. Sphingolipid-modulated exosome secretion promotes clearance of amyloid-beta by microglia. J Biol Chem. 2012;287:10977–89.
33. Bellingham SA, Guo BB, Coleman BM, Hill AF. Exosomes: vehicles for the transfer of toxic proteins associated with neurodegenerative diseases?. Front Physiol. 2012;3:124.
34. Chivet M, Hemming F, Pernet-Gallay K, Fraboulet S, Sadoul R. Emerging role of neuronal exosomes in the central nervous system. Front Physiol. 2012;3:145.
35. Frühbeis C, Fröhlich D, Krämer-Albers EM. Emerging roles of exosomes in neuron-glia communication. Front Physiol. 2012;3:119.
36. Lai CPK, Breakefield XO. Role of exosomes/microvesicles in the nervous system and use in emerging therapies. Front Physiol. 2012;3:228.
37. Lopez-Verrilli MA, Court FA. Transfer of vesicles from Schwann cells to axons: a novel mechanism of communication in the peripheral nervous system. Front Physiol. 2012;3:205.
38. Kalluri R, LeBleu VS. The biology, function, and biomedical applications of exosomes. Science. 2020;367:640.
39. Luarte A, Cisternas P, Caviedes A, Batiz LF, Lafourcade C, Wyneken U, et al. Astrocytes at the hub of the stress response: potential modulation of neurogenesis by miRNAs in astrocyte-derived exosomes. Stem Cell Int. 2017;2017:1719050.
40. Zheng TT, Pu JL, Chen YX, Guo ZY, Pan HY, Zhang L, et al. Exosomes secreted from HEK293-APP Swe/Ind cells impair the hippocampal neurogenesis. Neurotox Res. 2017;32:82–93.
41. Batiz LF, Castro MA, Burgos PV, Velasquez ZD, Munoz RI, Lafourcade CA, et al. Exosomes as novel regulators of adult neurogenic niches. Front Cell Neurosci. 2016;9:501.
42. Lafourcade C, Ramirez JP, Luarte A, Fernandez A, Wyneken U. MiRNAs in astrocyte-derived exosomes as possible mediators of neuronal plasticity. J Exp Neurosci. 2016;10:1–9.
43. Dalvi P, Sun B, Tang N, Pulliam L. Immune activated monocyte exosomes alter microRNAs in brain endothelial cells and initiate an inflammatory response through the TLR4/MyD88 pathway. Sci Rep.-Uk. 2017;7:9954.
44. Bălaşa A, Şerban G, Chinezu R, Hurghiş C, Tămaş F, Manu D. The involvement of exosomes in glioblastoma development, diagnosis, prognosis, and treatment. Brain Sci. 2020;10:553 https://doi.org/10.3390/brainsci10080553.
45. Dai J, Su Y, Zhong S, Cong L, Liu B, Yang J, et al. Exosomes: Key players in cancer and potential therapeutic strategy. Signal Transduct Target Ther. 2020;5:145 https://doi.org/10.1038/s41392-020-00261-0.
46. Banigan MG, Kao PF, Kozubek JA, Winslow AR, Medina J, Costa J, et al. Differential Expression of Exosomal microRNAs in Prefrontal Cortices of Schizophrenia and Bipolar Disorder Patients. PLoS One. 2013;8:e48814.
47. Song Z, Xu Y, Deng W, Zhang L, Zhu H, Yu P, et al. Brain derived exosomes are a double-edged sword in Alzheimer's disease. Front Mol Neurosci. 2020;13:79 https://doi.org/10.3389/fnmol.2020.00079.
48. Sardar Sinha M, Ansell-Schultz A, Civitelli L, Hildesjö C, Larsson M, et al. Alzheimer's disease pathology propagation by exosomes containing toxic amyloid-beta oligomers. Acta Neuropathol. 2018;136:745–61. https://doi.org/10.1007/s00401-018-1910-6.
49. Wang Y, Balaji V, Kaniyappan S, Krüger L, Irsen S, Tepper K, et al. The release and trans-synaptic transmission of Tau via exosomes. Mol Neurodegeneration. 2017;12:5. https://doi.org/10.1186/s13024-016-0143-y.
50. Stuendl A, Kunadt M, Kruse N, Bartels C, Moebius W, Danzer KM, et al. Induction of α-synuclein aggregate formation by CSF exosomes from patients with Parkinson's disease and dementia with Lewy bodies. Brain. 2016;139:1110–24. https://doi.org/10.1093/brain/awv395.
51. Sharma P, Mesci P, Carromeu C, McClatchy DR, Schiapparelli L, Yates JR 3rd, et al. Exosomes regulate neurogenesis and circuit assembly. Proc Natl Acad Sci. 2019;116:16086–94. https://doi.org/10.1073/pnas.1902513116.
52. Perets N, Hertz S, London M, Offen D. Intranasal administration of exosomes derived from mesenchymal stem cells ameliorates autistic-like behaviors of BTBR mice. Mol Autism. 2018;9:57. https://doi.org/10.1186/s13229-018-0240-6.
53. Perets N, Oron O, Herman S, Elliott E, Offen D. Exosomes derived from mesenchymal stem cells improved core symptoms of genetically modified mouse model of autism Shank3B. Mol Autism. 2020;11:65. https://doi.org/10.1186/s13229-020-00366-x.
54. Cerneckis J, Cai H, Shi Y. Induced pluripotent stem cells (iPSCs): Molecular mechanisms of induction and applications. Signal Transduct Target Ther. 2024;9:112 https://doi.org/10.1038/s41392-024-01809-3.
55. Notaras M, Lodhi A, Fang H, Greening D, Colak D. The proteomic architecture of schizophrenia iPSC-derived cerebral organoids reveals alterations in GWAS and neuronal development factors. Transl Psychiatry. 2021;11:541. https://doi.org/10.1038/s41398-021-01446-7.
56. Notaras M, Lodhi A, Dündar F, Collier P, Sayles NM, Tilgner H, et al. Schizophrenia is defined by cell-specific neuropathology and multiple neurodevelopmental mechanisms in patient-derived cerebral organoids. Mol Psychiatry. 2022;27:1416–34. https://doi.org/10.1038/s41380-021-01388-9.
57. Stankovic IN, Colak D. Prenatal drugs and their effects on the developing brain: Insights from three-dimensional human organoids. Front Neurosci. 2022;16:848648. https://doi.org/10.3389/fnins.2022.848648.
58. Stankovic I, Notaras M, Wolujewicz P, Lu T, Lis R, Ross ME, et al. Schizophrenia endothelial cells exhibit higher permeability and altered angiogenesis patterns in patient-derived organoids. Transl Psychiatry. 2024;14:53. https://doi.org/10.1038/s41398-024-02740-2.
59. Velasco S, Kedaigle AJ, Simmons SK, Nash A, Rocha M, Quadrato G, et al. Individual brain organoids reproducibly form cell diversity of the human cerebral cortex. Nature. 2019;570:523–7. https://doi.org/10.1038/s41586-019-1289-x.
60. Théry C, Witwer KW, Aikawa E, Alcaraz MJ, Anderson JD, Andriantsitohaina R, et al. Minimal information for studies of extracellular vesicles 2018 (MISEV2018): a position statement of the international society for extracellular vesicles and update of the MISEV2014 guidelines. J Extracell Vesicles. 2018;7:1535750. https://doi.org/10.1080/20013078.2018.1535750.
61. Mathieu M, Névo N, Jouve M, Valenzuela JI, Maurin M, Verweij FJ, et al. Specificities of exosome versus small ectosome secretion revealed by live intracellular tracking of CD63 and CD9. Nat Commun. 2021;12:4389. https://doi.org/10.1038/s41467-021-24384-2.
62. Jung MK, Mun JY. Sample Preparation and Imaging of Exosomes by Transmission Electron Microscopy. J Visualized Experiments: JoVE. 2018;4:56482 https://doi.org/10.3791/56482.
63. Tsai HF, Shen AQ. Impact of dcEF on microRNA profiles in glioblastoma and exosomes using a novel microfluidic bioreactor. Biomicrofluidics. 2024;18:064106. https://doi.org/10.1063/5.0228901.
64. Shimada Y, Yoshioka Y, Kudo Y, Mimae T, Miyata Y, Adachi H, et al. Extracellular vesicle-associated microRNA signatures related to lymphovascular invasion in early-stage lung adenocarcinoma. Sci Rep. 2023;13:4823. https://doi.org/10.1038/s41598-023-32041-5tsa.
65. Li YY, Liu H, Feng JL, Tian WY, Du J, Zhang LP. Engineered exosomes restore miR-508-5p expression in uterine corpus endometrial carcinoma and reduce tumor progression and metastasis by targeting DLL3. Front Oncol. 2025;15:1532564. https://doi.org/10.3389/fonc.2025.1532564.
66. Siniscalco D, Giordano A, Galderisi U. Novel insights in basic and applied stem cell therapy. J Cell Physiol. 2012;227:2283–6. https://doi.org/10.1002/jcp.22945.
67. Siniscalco D, Bradstreet JJ, Sych N, Antonucci N. Perspectives on the use of stem cells for autism treatment. Stem Cell Int. 2013;2013:262438. https://doi.org/10.1155/2013/262438.
68. Siniscalco D, Sapone A, Cirillo A, Giordano C, Maione S, Antonucci N. Autism spectrum disorders: Is mesenchymal stem cell personalized therapy the future?. J Biomedicine Biotechnol. 2012;2012:480289. https://doi.org/10.1155/2012/480289.
69. Han C, Sun X, Liu L, Jiang H, Shen Y, Xu X, et al. Exosomes and their therapeutic potentials of stem cells. Stem Cell Int. 2016;2016:7653489. https://doi.org/10.1155/2016/7653489.
70. Kim HJ, Kim G, Lee J, Lee Y, Kim JH. Secretome of stem cells: Roles of extracellular vesicles in diseases, stemness, differentiation, and reprogramming. Tissue Eng Regen Med. 2022;19:19–33. https://doi.org/10.1007/s13770-021-00406-4.
71. Xia J, Minamino S, Kuwabara K, Arai S. Stem cell secretome as a new booster for regenerative medicine. Biosci Trends. 2019;13:299–307. https://doi.org/10.5582/bst.2019.01226.

72. Courchesne E, Taluja V, Nazari S, Aamodt CM, Pierce K, Duan K, et al. Embryonic origin of two ASD subtypes of social symptom severity: The larger the brain cortical organoid size, the more severe the social symptoms. Mol Autism. 2024;15:22. https://doi.org/10.1186/s13229-024-00602-8.
73. Urresti J, Zhang P, Moran-Losada P, Yu NK, Negraes PD, Trujillo CA, et al. Cortical organoids model early brain development disrupted by 16p11.2 copy number variants in autism. Mol Psychiatry. 2021;26:7560–80. https://doi.org/10.1038/s41380-021-01243-6.
74. Vaccarino FM, Smith KM. Increased brain size in autism—what it will take to solve a mystery. Biol Psychiatry. 2009;66:313–5. https://doi.org/10.1016/j.biopsych.2009.06.013.
75. Birtele M, Del Dosso A, Xu T, Nguyen T, Wilkinson B, Hosseini N, et al. Non-synaptic function of the autism spectrum disorder-associated gene SYNGAP1 in cortical neurogenesis. Nat Neurosci. 2023;26:2090–103. https://doi.org/10.1038/s41593-023-01477-3.
76. Forero A, Pipicelli F, Moser S, Baumann N, Grätz C, Gonzalez Pisfil M, et al. Extracellular vesicle-mediated trafficking of molecular cues during human brain development. Cell Rep. 2024;43:114755. https://doi.org/10.1016/j.celrep.2024.114755.
77. Ji X, Zhou S, Wang N, Wang J, Wu Y, Duan Y, et al. Cerebral-organoid-derived exosomes alleviate oxidative stress and promote LMX1A-dependent dopaminergic differentiation. Int J Mol Sci. 2023;24:11048 https://doi.org/10.3390/ijms241311048.
78. Skottvoll FS, Berg HE, Bjørseth K, Lund K, Roos N, Bekhradnia S, et al. Ultracentrifugation versus kit exosome isolation: NanoLC-MS and other tools reveal similar performance biomarkers, but also contaminations. Future Sci OA. 2018;5:FSO359. https://doi.org/10.4155/fsoa-2018-0088.
79. Ansari FJ, Tafti HA, Amanzadeh A, Rabbani S, Shokrgozar MA, Heidari R, et al. Comparison of the efficiency of ultrafiltration, precipitation, and ultracentrifugation methods for exosome isolation. Biochem Biophysics Rep. 2024;38:101668. https://doi.org/10.1016/j.bbrep.2024.101668.
80. Brennan K, Martin K, FitzGerald SP, et al. A comparison of methods for the isolation and separation of extracellular vesicles from protein and lipid particles in human serum. Sci Rep. 2020;10:1039. https://doi.org/10.1038/s41598-020-57497-7.
81. Patel GK, Khan MA, Zubair H, Srivastava SK, Khushman M, Singh S, et al. Comparative analysis of exosome isolation methods using culture supernatant for optimum yield, purity, and downstream applications. Sci Rep. 2019;9:5335. https://doi.org/10.1038/s41598-019-41800-2.
82. Wei Z, Batagov AO, Schinelli S, Wang J, Yang W, et al. Coding and noncoding landscape of extracellular RNA released by human glioma stem cells. Nat Commun. 2017;8:1145.
83. Nogay NH, Walton J, Roberts KM, Nahikian-Nelms M, Witwer AN. The effect of the low FODMAP diet on gastrointestinal symptoms, behavioral problems, and nutrient intake in children with autism spectrum disorder: A randomized controlled pilot trial. J Autism Dev Disord. 2021;51:2800–11. https://doi.org/10.1007/s10803-020-04717-8.
84. Frere SG, Chang-Ileto B, Di Paolo G. Role of phosphoinositides at the neuronal synapse. Sub-Cell Biochem. 2012;59:131–75. https://doi.org/10.1007/978-94-007-3015-1_5.
85. Tariq K, Luikart BW. Striking a balance: PIP2 and PIP3 signaling in neuronal health and disease. Exploration Neuroprotective Ther. 2021;1:86–100. https://doi.org/10.37349/ent.2021.00008.
86. Pegtel DM, Cosmopoulos K, Thorley-Lawson DA, van Eijndhoven MA, Hopmans ES, Lindenberg JL, et al. Functional delivery of viral miRNAs via exosomes. Proc Natl Acad Sci USA. 2010;107:6328–33. https://doi.org/10.1073/pnas.0914843107.
87. Zheng D, Huo M, Li B, Wang W, Piao H, Wang Y, et al. The role of exosomes and exosomal microRNA in cardiovascular disease. Front Cell Dev Biol. 2021;8:616161. https://doi.org/10.3389/fcell.2020.616161.
88. Gu C, Mo W, Wang K, Gao M, Chen J, Zhang F, et al. Exosomal miR-370-3p increases the permeability of blood-brain barrier in ischemia/reperfusion stroke of brain by targeting MPK1. Aging. 2023;15:1931–43. https://doi.org/10.18632/aging.204573.
89. Wang Y, Yu S, Li M. Neurovascular crosstalk and cerebrovascular alterations: an underestimated therapeutic target in autism spectrum disorders. Front Cell Neurosci. 2023;17:1226580. https://doi.org/10.3389/fncel.2023.1226580.
90. Soutschek M, Lo Bianco A, Wentinck K, Galkin S, Wüst T, Colameo D, et al. A human-specific microRNA controls the timing of excitatory synaptogenesis. BioRxiv: 2023.10.04.560889 [Preprint] 2025. Available from: https://doi.org/10.1101/2023.10.04.560889.
91. An X, Ge J, Guo H, Mi H, Zhou J, Liu Y, et al. Overexpression of miR-4286 is an unfavorable prognostic marker in individuals with non-small cell lung cancer. J Cell Biochem. 2019;120:17573–83. https://doi.org/10.1002/jcb.29024.
92. Erbescu A, Papuc SM, Budisteanu M, Arghir A, Neagu M. Re-emerging concepts of immune dysregulation in autism spectrum disorders. Front Psychiatry. 2022;13:1006612. https://doi.org/10.3389/fpsyt.2022.1006612.
93. Schmidt MF, Gan ZY, Komander D, Dewson G. Ubiquitin signalling in neurodegeneration: mechanisms and therapeutic opportunities. Cell Death Differ. 2021;28:570–90. https://doi.org/10.1038/s41418-020-00706-7.
94. Bousman CA, Luza S, Mancuso SG, Kang D, Opazo CM, Mostaid MS, et al. Elevated ubiquitinated proteins in brain and blood of individuals with schizophrenia. Sci Rep. 2019;9:2307. https://doi.org/10.1038/s41598-019-38490-1.
95. Etzioni A, Ciechanover A, Pikarsky E. Immune defects caused by mutations in the ubiquitin system. J Allergy Clin Immunol. 2017;139:743–53. https://doi.org/10.1016/j.jaci.2016.11.031.
96. Louros SR, Osterweil EK. Perturbed proteostasis in autism spectrum disorders. J Neurochemistry. 2016;139:1081–92. https://doi.org/10.1111/jnc.13723.
97. Kasherman MA, Premarathne S, Burne THJ, Wood SA, Piper M. The ubiquitin system: A regulatory hub for intellectual disability and autism spectrum disorder. Mol Neurobiol. 2020;57:2179–93. https://doi.org/10.1007/s12035-020-01881-x.
98. Crider A, Pandya CD, Peter D, Ahmed AO, Pillai A. Ubiquitin-proteasome dependent degradation of GABAAα1 in autism spectrum disorder. Mol Autism. 2014;5:45. https://doi.org/10.1186/2040-2392-5-45.
99. Vinci M, Treccarichi S, Galati Rando R, Musumeci A, Todaro V, Federico C, et al. A de novo ARIH2 gene mutation was detected in a patient with autism spectrum disorders and intellectual disability. Sci Rep. 2024;14:15848. https://doi.org/10.1038/s41598-024-66475-2.
100. Tener SJ, Lin Z, Park SJ, Oraedu K, Ulgherait M, Ven Beek E, et al. Neuronal knockdown of Cullin3 as a drosophila model of autism spectrum disorder. Sci Rep. 2024;14:1541. https://doi.org/10.1038/s41598-024-51657-9.
101. Vintermist A, Böhm S, Sadeghifar F, Louvet E, Mansén A, Percipalle P, et al. The chromatin remodelling complex B-WICH changes the chromatin structure and recruits histone acetyl-transferases to active rRNA genes. PLoS One. 2011;6:e19184 https://doi.org/10.1371/journal.pone.0019184.
102. Astorkia M, Liu Y, Pedrosa EM, Lachman HM, Zheng D. Molecular and network disruptions in neurodevelopment uncovered by single-cell transcriptomics analysis of CHD8 heterozygous cerebral organoids. Heliyon. 2024;10:e34862. https://doi.org/10.1016/j.heliyon.2024.e34862.
103. Needleman LA, McAllister AK. The major histocompatibility complex and autism spectrum disorder. Dev Neurobiol. 2012;72:1288–1301. https://doi.org/10.1002/dneu.2204.
104. Wan L, Yang G, Yan Z. Identification of a molecular network regulated by multiple ASD high risk genes. Hum Mol Genet. 2024;33:1176–85. https://doi.org/10.1093/hmg/ddae058.
105. Santini E, Huynh TN, MacAskill AF, Carter AG, Pierre P, Ruggero D, et al. Exaggerated translation causes synaptic and behavioral aberrations associated with autism. Nature. 2013;493:411–5. https://doi.org/10.1038/nature11782.
106. Bear M, Dölen G, Osterweil E, Nagarajan N. Fragile X: translation in action. Neuropsychopharmacol. 2018;33:84–87.
107. Hooshmandi M, Wong C, Khoutorsky A. Dysregulation of translational control signaling in autism spectrum disorders. Cell Signal. 2020;75:109746. https://doi.org/10.1016/j.cellsig.2020.109746.
108. Chabout J, Sarkar A, Patel SR, Radden T, Dunson DB, Fisher SE, et al. A Foxp2 mutation implicated in human speech deficits alters sequencing of ultrasonic vocalizations in adult male mice. Front Behav Neurosci. 2016;10:197 https://doi.org/10.3389/fnbeh.2016.00197.
109. Allan AM, Liang X, Luo Y, Pak C, Li X, Szulwach KE, et al. The loss of methyl-CpG binding protein 1 leads to autism-like behavioral deficits. Hum Mol Genet. 2008;17:2047–57. https://doi.org/10.1093/hmg/ddn102.
110. Allen M, Huang BS, Notaras MJ, Lodhi A, Barrio-Alonso E, Lituma PJ, et al. Astrocytes derived from ASD individuals alter behavior and destabilize neuronal activity through aberrant Ca2+ signaling. Mol Psychiatry. 2022;27:2470–84. https://doi.org/10.1038/s41380-022-01486-x.
111. Bojmar L, Kim HS, Tobias GC, Pelissier Vatter FA, Lucotti S, Gyan KE, et al. Extracellular vesicle and particle isolation from human and murine cell lines, tissues, and bodily fluids. STAR Protoc. 2020;2:100225. https://doi.org/10.1016/j.xpro.2020.100225.
112. Wang G, Li J, Bojmar L, Chen H, Li Z, Tobias GC, et al. Tumour extracellular vesicles and particles induce liver metabolic dysfunction. Nature. 2023;618:374–82. https://doi.org/10.1038/s41586-023-06114-4.

ACKNOWLEDGEMENTS

We thank the Genomics Resources Core Facility, the Proteomics Resource Core Facility, and Microscopy and Imaging Core Facility at Weill Cornell Medicine for their assistance in conducting the RNA sequencing, proteomics and TEM imaging, respectively. The authors would also like to thank Dr. David Lyden and Dr. Haiying Zhang for their assistance in conducting the NTA analysis and for their helpful discussions about EVs.

AUTHOR CONTRIBUTIONS

IS designed and performed most of the experiments, analyzed the data, and wrote the manuscript with help from DC. PS and PW analyzed RNA sequencing data and generated the plots. JC, AR, and DG analyzed proteomics data and generated the plots. This research was funded by the National Institute of Mental Health, National Institutes of Health, grant number R21MH131985-01A1.

COMPETING INTERESTS

The authors report no conflict of interest or commercial interests related to the manuscript.

ETHICS APPROVAL AND CONSENT TO PARTICIPATE

The specimens coming from the Coriell CIRM collection and the NIMH Repository iPSC collection are consented broadly for general research use of the deidentified biospecimens and clinical data.

ADDITIONAL INFORMATION

Supplementary information The online version contains supplementary material available at https://doi.org/10.1038/s41398-025-03607-w.

Correspondence and requests for materials should be addressed to Dilek Colak.